Effective-medium theory of percolation on central-force elastic networks. II. Further results

E. J. Garboczi* and M. F. Thorpe
Department of Physics and Astronomy, Michigan State University, East Lansing, Michigan 48824-1116
(Received 21 January 1985)

The effective-medium theory developed in a previous paper for elastic networks with a fraction p of the bonds present is extended to networks which have central forces of arbitrary range. The results are illustrated by studying a square lattice with a fraction p_1 of nearest-neighbor bonds present and a fraction p_2 of next-nearest-neighbor bonds present. We show that effective-medium theory gives an excellent description of the elastic properties of the networks. An argument using constraints is used to show that the network loses its elastic properties when $p_1+p_2<1$ and that the number of zero-frequency modes depends only on p_1+p_2. We construct flow diagrams to show that a line of fixed points exists when $p_1+p_2=1$, along which the ratio of elastic constants attains a universal value that depends on p_1 but *not* on the spring constants. The simulations show no significant deviations from the effective-medium results.

I. INTRODUCTION

In a previous paper[1] (henceforth referred to as I) the authors developed an effective-medium theory (EMT) for networks with nearest-neighbor central forces α, in which a fraction p of the bonds were present. In that work it was shown that the elastic moduli C_{ij} for the triangular net (which has dimensionality $d=2$ and $z=6$ nearest neighbors) were given by

$$C_{44}=\tfrac{1}{3}C_{11}=\frac{\sqrt{3}}{4}\alpha_m \ , \tag{1}$$

where

$$\alpha_m=\frac{p-p_{\rm cen}}{1-p_{\rm cen}} \tag{2}$$

and

$$p_{\rm cen}=2d/z=\tfrac{2}{3} \ . \tag{3}$$

Effective-medium theory always gets the initial slope (for small $1-p$) correct and in I it was shown that the elastic constants $C_{ij}=0$ for $p<p_{\rm cen}$. By comparing Eqs. (1)—(3) with numerical simulations, it was found that effective-medium theory did remarkably well. This is largely due to the fact that the transition takes place close to the EMT prediction $p_{\rm cen}=\frac{2}{3}$. Indeed no significant deviations from EMT were found in I although such deviations probably exist in the "critical region" around $p_{\rm cen}$. Similar conclusions hold for the fcc lattice, with $d=3$ and $z=12$ substituted into Eq. (3), to give $p_{\rm cen}=\frac{1}{2}$.

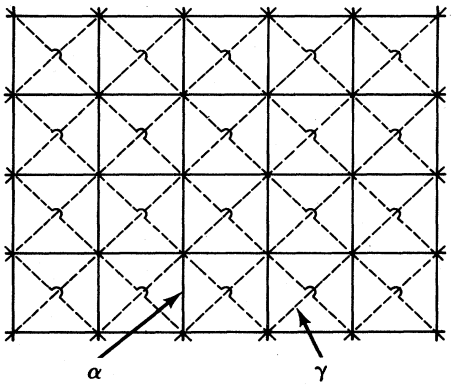

FIG. 1. Piece of the square net with nearest-neighbor bonds (solid lines) with force constant α and next-nearest-neighbor bonds (dashed lines) with force constant γ.

In this paper we study a model of *greater complexity* to see if EMT can still provide a good description of the simulations. The model we study is a square lattice with nearest-neighbor central forces α, and next-nearest-neighbor forces γ as shown in Fig. 1. We randomly remove α-type bonds with probability $(1-p_1)$ and γ-type bonds with probability $(1-p_2)$. In the next section we summarize the properties of the undiluted system. In Sec. III we use the *constraints method*[2] to locate the critical line in the (p_1,p_2) plane. In Sec. IV we derive the EMT equations and in Sec. V we compare the EMT results to simulations. In the conclusions we discuss the *universal* nature of the fixed points that are obtained both in EMT and in the simulations.

II. PURE SYSTEM

The system under consideration is illustrated in Fig. 1 and described by the potential,

$$V=\frac{\alpha}{2}\sum_{\langle ij\rangle}[(\mathbf{u}_i-\mathbf{u}_j)\cdot\hat{\mathbf{r}}_{ij}]^2p_{1,ij} + \frac{\gamma}{2}\sum_{\langle ij\rangle}[(\mathbf{u}_i-\mathbf{u}_j)\cdot\hat{\mathbf{r}}_{ij}{}']^2p_{2,ij} \ , \tag{4}$$

where the first term is associated with the horizontal and vertical bonds in Fig. 1 and the second term with the bonds at 45° to the horizontal. The angular brackets

under the summations are to signify that each interaction is counted only once. The first sum goes over nearest neighbors, designated by unit vectors $\hat{\mathbf{r}}_{ij}$, and the second sum goes over next-nearest neighbors, designated by unit vectors $\hat{\mathbf{r}}'_{ij}$. The *independent* probabilities $p_{1,ij}$ and $p_{2,ij}$ are associated with nearest-neighbor and next-nearest-neighbor bonds, respectively, and are 0,1 with probability $(1-p_1),p_1$ for nearest neighbors and $(1-p_2),p_2$ for next-nearest neighbors. The $\mathbf{u}_i$ are the displacements from equilibrium of the mass points, all with mass m.

For the pure system all the $p_{1,ij}=p_{2,ij}=1$ and the equations of motion define the dynamical matrix $\mathbf{D}_{ij}$ via

$$m\omega^2\mathbf{u}_i=\sum_j \mathbf{D}_{ij}\mathbf{u}_j \ . \tag{5}$$

Of more interest is the Fourier transform of the dynamical matrix,

$$\mathbf{D}(\mathbf{k})=\sum_{i,j}\mathbf{D}_{ij}\exp[i\mathbf{k}\cdot(\mathbf{r}_j-\mathbf{r}_i)] \tag{6}$$

$$=\alpha\sum_{\delta}[1-\exp(ia\mathbf{k}\cdot\hat{\delta})]\hat{\delta}\hat{\delta}$$

$$+\gamma\sum_{\delta'}[1-\exp(ib\mathbf{k}\cdot\hat{\delta}')]\hat{\delta}'\hat{\delta}' \ , \tag{7}$$

where the nearest-neighbor separation is $a=b/\sqrt{2}$ and $\hat{\delta}$ is any one of the four possible $\hat{\mathbf{r}}_{ij}$ and $\hat{\delta}'$ is any one of the four possible $\hat{\mathbf{r}}_{ij}'$. Associating x and y Cartesian coordinates with the horizontal and vertical directions in Fig. 1, the dynamical matrix may be written as

$$\mathbf{D}(\mathbf{k})=\begin{bmatrix} 2\alpha[1-\cos(k_x a)]+2\gamma[1-\cos(k_x a)\cos(k_y a)] & 2\gamma\sin(k_x a)\sin(k_y a) \\ 2\gamma\sin(k_x a)\sin(k_y a) & 2\alpha[1-\cos(k_y a)]+2\gamma[1-\cos(k_x a)\cos(k_y a)] \end{bmatrix} . \tag{8}$$

The normal modes are longitudinal (L) and transverse (T) along the principal directions and are given along (1,0) by

$$m\omega_T^2=2\gamma[1-\cos(k_x a)] \ ,$$
$$m\omega_L^2=2(\alpha+\gamma)[1-\cos(k_x a)] \ , \tag{9}$$

and along (1,1), where $k_x=k_y$ by

$$m\omega_T^2=2\alpha[1-\cos(k_x a)] \ ,$$
$$m\omega_L^2=2\alpha[1-\cos(k_x a)]+2\gamma[1-\cos(2k_x a)] \ . \tag{10}$$

Using conventional elasticity theory,[3] the three elastic moduli can be extracted from (9) and (10) in the long-wavelength limit:

$$C_{11}=\alpha+\gamma \ , \tag{11}$$

$$C_{12}=C_{44}=\gamma \ . \tag{12}$$

Equation (12) is a manifestation of the Cauchy relation[4] which states that $C_{12}=C_{44}$ for systems with central forces only in which *every atom* is at a center of symmetry. The maximum frequency in the system ($\omega_{\max}$) is given by

$$m\omega_{\max}^2=4(\alpha+\gamma) \ . \tag{13}$$

III. CONSTRAINTS METHOD

This is a very powerful and simple method that can be used to estimate where the phase transition takes place.[1,2] The number of zero-frequency modes ($2fN$) is equal to the number of degrees of freedom ($2N$) minus the number of constraints [$2N(p_1+p_2)$] where N is the number of atoms. Hence

$$f=1-(p_1+p_2) \tag{14}$$

and the transition takes place when $f=0$ or

$$p_1^c+p_2^c=1 \ , \tag{15}$$

where the superscripts c denote the values at the transition. The quantity f is the fraction of modes that have zero frequency.

We have done simulations to test Eq. (14). Periodic networks with $20\times20=400$ atoms were constructed with a fraction p_1 of the nearest-neighbor bonds present and a fraction p_2 of the next-nearest-neighbor bonds present. The number of modes at zero frequency were calculated by constructing the dynamical matrix and finding the total number of eigenfrequencies with $\omega^2<\epsilon$ where ϵ is very small (we took $\epsilon\sim10^{-5}\omega_{\max}^2$). This was done for a number of samples along tracks 1 and 3 in Fig. 2. Track 1 is characterized by $p_1=p_2$ and track 3 by $p_1=2.37p_2$ (the reasons for the choice of the somewhat curious number 2.37 are explained in Sec. V). Because Eq. (14) predicts

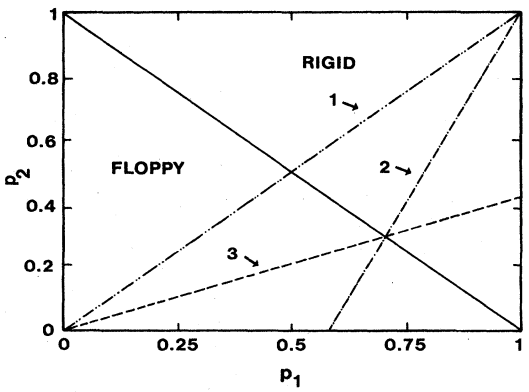

FIG. 2. Showing the rigid and floppy regions in the (p_1,p_2) plane. The dividing line between these two phases is given by Eq. (15). Three "tracks" are shown and numbered in the plane.

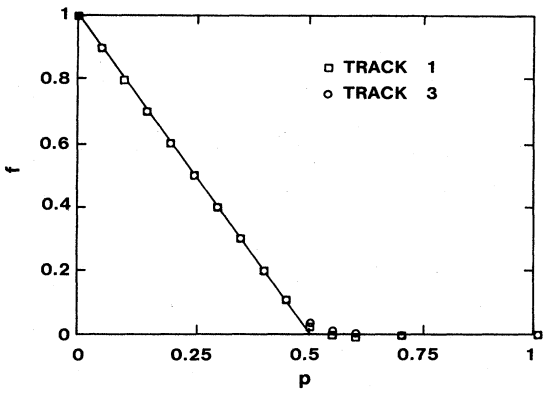

FIG. 3. The fraction of zero-frequency modes (f) as a function of $p=\frac{1}{2}(p_1+p_2)$ along two different tracks (see Fig. 2). The straight line represents (14) and the symbols are the result of simulations averaged over three ($20\times20=400$)-atom networks.

that the results should only depend on the sum p_1+p_2 and not on p_1 and p_2 individually, we plotted the results for f against $p=\frac{1}{2}(p_1+p_2)$ as shown in Fig. 3. It can be seen that the results from both tracks do fall very close to the result (14). The rounding close to $p^c=\frac{1}{2}(p_1^c+p_2^c)=\frac{1}{2}$ is partially due to finite-size effects. Some of the rounding is intrinsic as small floppy inclusions are present in the rigid percolating region at the transition.[2] More careful simulations are required in this region, as a function of sample size, in order to study these effects.

As in I, we again see the power of the constraints method in locating the critical point. The reason that it is much more successful in *vector* rather than *scalar* percolation problems is not understood.[5]

IV. EFFECTIVE-MEDIUM THEORY

In I an effective-medium theory (or coherent-potential approximation) was developed for the case where all the bonds were identical. The same result was obtained by two distinct methods. In the static method, the *average strain* around a "wrong bond" in an effective medium was set equal to zero. This condition determined the effective-medium parameter. In the second method, the *average T matrix* was set equal to zero for scattering from a wrong bond in an effective medium. Again this condition determined the effective-medium parameter. The results found in I can be summarized as

$$\frac{\alpha_m}{\alpha}=\frac{p-a^*}{1-a^*}\ , \tag{16}$$

$$a^*=\frac{2\alpha_m}{Nz}\sum_{k,\delta}\mathrm{Tr}\{[1-\exp(ia\mathbf{k}\cdot\hat{\boldsymbol{\delta}})]\hat{\boldsymbol{\delta}}\hat{\boldsymbol{\delta}}\cdot\mathbf{D}^{-1}(\mathbf{k})\}\ , \tag{17}$$

$$\mathbf{D}(\mathbf{k})=\alpha_m\sum_{\delta}[1-\exp(ia\mathbf{k}\cdot\hat{\boldsymbol{\delta}})]\hat{\boldsymbol{\delta}}\hat{\boldsymbol{\delta}}\ . \tag{18}$$

These equations determine the effective-medium parameter $\alpha_m(p)$ and hence the elastic moduli can be found. The number of nearest neighbors is z and there are N sites. For the case of only a single type of bond, the sum in (17) can be done explicitly to give $a^*=2d/z$. The transition takes place when $p_{\mathrm{cen}}=a^*=2d/z$.

These equations are easily generalized to an arbitrary number of central forces which can have an arbitrary range. Inclusion of angular forces is much more difficult. In the present case we must introduce *two* effective-medium parameters α_m and γ_m. Because the two kinds of bonds are present randomly, α_m and γ_m can be determined separately by either of the methods in I. The results are

$$\frac{\alpha_m}{\alpha}=\frac{p_1-a_1^*}{1-a_1}\ , \tag{19}$$

$$\frac{\gamma_m}{\gamma}=\frac{p_2-a_2^*}{1-a_2}\ , \tag{20}$$

$$a_1^*=\frac{2\alpha_m}{Nz_1}\sum_{k,\delta}\mathrm{Tr}\{[1-\exp(ia\mathbf{k}\cdot\hat{\boldsymbol{\delta}})]\hat{\boldsymbol{\delta}}\hat{\boldsymbol{\delta}}\cdot\mathbf{D}^{-1}(\mathbf{k})\}\ , \tag{21}$$

$$a_2^*=\frac{2\gamma_m}{Nz_2}\sum_{k,\delta'}\mathrm{Tr}\{[1-\exp(ib\mathbf{k}\cdot\hat{\boldsymbol{\delta}}')]\hat{\boldsymbol{\delta}}'\hat{\boldsymbol{\delta}}'\cdot\mathbf{D}^{-1}(\mathbf{k})\}\ , \tag{22}$$

and the dynamical matrix is given by (7) with α,γ replaced by α_m,γ_m. The numbers of nearest neighbors z_1 and next-nearest neighbors z_2 are both 4 in the square net. The equations for α_m,γ_m are coupled through the dynamical matrix. In the present case a_1^* and a_2^* *cannot* be evaluated in closed form. The transition takes place when

$$p_1^c=a_1^*\ \text{ and }\ p_2^c=a_2^*\ . \tag{23}$$

It can easily be seen from (21) and (22) that

$$a_1^*+a_2^*=1\ , \tag{24}$$

so that $p_1^c+p_2^c=1$ as found previously using the constraints argument leading to (15). Because of the result (24) it is only necessary to compute a_1^* which can be written explicitly as

$$a_1^*=\frac{1}{\pi^2}\int_0^\pi\int_0^\pi dx\,dy\,\frac{2(1-r_m)-(2+r_m)(c_x+c_y)+(2+r_mc_x+r_mc_y)c_xc_y}{1+2r_m+r_m^2(c_x-c_y)^2+(1-2r_m)c_xc_y-(1+r_m-r_mc_xc_y)(c_x+c_y)}\ , \tag{25}$$

where $r_m=\gamma_m/\alpha_m$, $c_x=\cos(k_xa)$, and $c_y=\cos(k_ya)$. This integral was evaluated using a 22×22 point Gaussian quadrature routine. The results are discussed in the next section.

We note that these results can easily be extended to more distant central-force interactions. If there are z_i bonds from a given atom to equivalent neighbors in the ith shell, which are each randomly present with probability p_i, and if there is a total of r such sets of neighbors, then the EMT will contain r equations such as (19) and (21) which are effectively coupled through the appropriate dynamical matrix. In an obvious generalization of previ-

ous notation, these equations are

$$\frac{\alpha_{im}}{\alpha_i}=\frac{p_i-a_i^*}{1-a_i^*}\ , \tag{26}$$

$$a_i^*=\frac{2\alpha_{im}}{Nz_i}\sum_{k,\delta_i}\mathrm{Tr}\{[1-\exp(ia_i\mathbf{k}\cdot\hat{\delta}_i)]\hat{\delta}_i\hat{\delta}_i\cdot\mathbf{D}^{-1}(\mathbf{k})\}\ , \tag{27}$$

$$\mathbf{D}(\mathbf{k})=\sum_{i=1}^{r}\alpha_{im}\sum_{\delta_i}[ia_i\mathbf{k}\cdot\hat{\delta}_i)]\hat{\delta}_i\hat{\delta}_i\ , \tag{28}$$

where a_i (not to be confused with a_i^*) is the distance to the neighbors in the ith shell and $\hat{\delta}_i$ are unit vectors to atoms in the ith shell. The following sum rule is easily proved from (27) and (28):

$$\sum_{i=1}^{r}z_ia_i^*=2d\ , \tag{29}$$

leading to

$$\sum_{i=1}^{r}z_ip_i^c=2d\ , \tag{30}$$

which defines the critical surface. We note that this same result is also obtained (more easily) by a simple generalization of the constraints argument in the preceding section.

V. RESULTS

We present results for the elastic moduli along track 1 (with $p_1=p_2$) and track 2 [with $(1-p_2)=2.37(1-p_1)$] in the (p_1,p_2) plane as shown in Fig. 2. In all cases the results are displayed as a function of $p=\frac{1}{2}(p_1+p_2)$ so that there is a *common* critical value $p^c=0.5$.

The simulations were performed as described in I using $(40\times40=1600)$-atom networks.[6] A suitable external strain was used to redefine the vectors that define the periodically repeated unit "supercell" containing 1600 atoms. The atoms were moved towards positions where there is no force on them. The elastic modulus was extracted by measuring the total strain energy in the system. In this way we computed C_{11}, C_{44}, and the bulk modulus $\frac{1}{2}(C_{11}+C_{12})$. The results for C_{11} were averaged over the two directions. Because of rotational invariance there is only a single C_{44} for each sample.[1]

In Fig. 4 we show results for C_{12} and C_{44}. Within the error bars of the simulations they appear to be equal. They should be equal for the *pure system* ($p_1=p_2=1$) as shown by Eq. (12). This is because the conditions under which Cauchy's theorem is usually stated[4] are satisfied: The potential contains only central forces and every site is at a center of inversion symmetry. When bonds are cut, sites are no longer centers of inversion symmetry and yet surprisingly $C_{12}=C_{44}$ still appears to hold (see Fig. 4). We suspect that Cauchy's theorem may be true under more general conditions than have heretofore been proved. In particular, it appears that macroscopic inversion symmetry may be sufficient and microscopic inversion symmetry is not required.

In Fig. 5 we show the results of simulations for C_{11} and

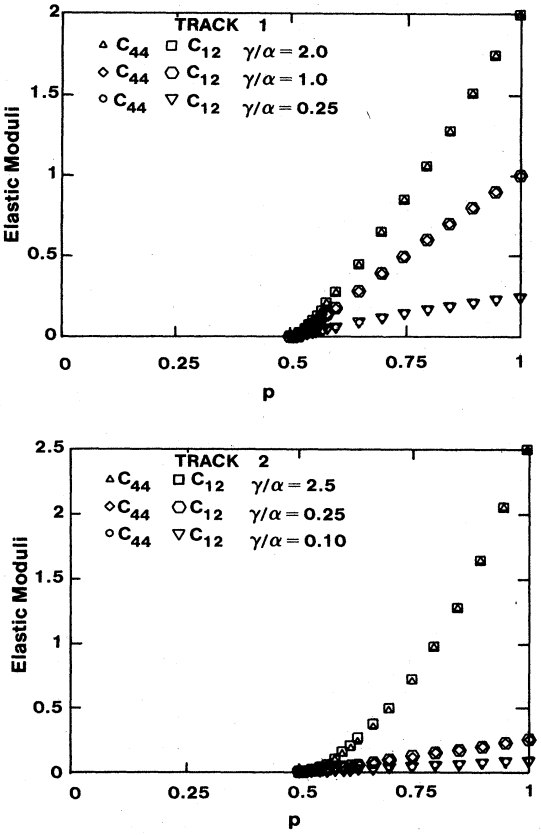

FIG. 4. Showing results for three initial values of γ/α from simulations along two tracks (see Fig. 2) averaged over five $(40\times40=1600)$-atom networks for C_{12} and C_{44}. The elastic moduli are in units where $\alpha=1$ and $p=\frac{1}{2}(p_1+p_2)$.

C_{44}. Note that C_{11}, C_{12}, and C_{44} all go to zero at $p^c=0.5$ to within the accuracy of the simulations.

From the effective-medium equations, we extract α_m and γ_m and hence [see Eqs. (11) and (12)] we obtain $C_{12}=C_{44}=\gamma_m$ and $C_{11}=\alpha_m+\gamma_m$. The effective-medium equations, by nature, predict $C_{11}=C_{44}$. The fits

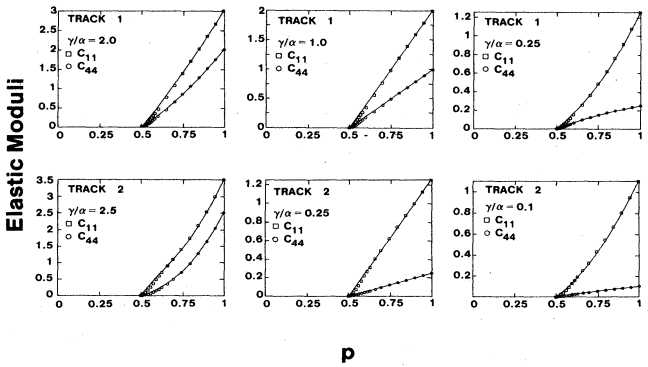

FIG. 5. Showing the results for three initial values of γ/α along two different tracks (see Fig. 2). The points are from simulations averaged over five $(40\times40=1600)$-atom networks. The elastic moduli are in units where $\alpha=1$ and $p=\frac{1}{2}(p_1+p_2)$.

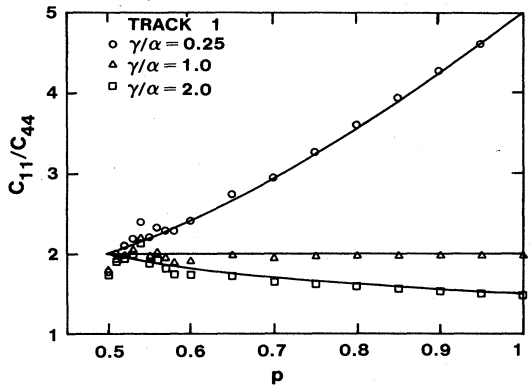

FIG. 6. Flow diagram along track 1 (where $p_1=p_2$) showing that C_{11}/C_{44} becomes independent of γ/α at the critical point. The solid lines are from EMT and the points are from the simulations shown in Fig. 5.

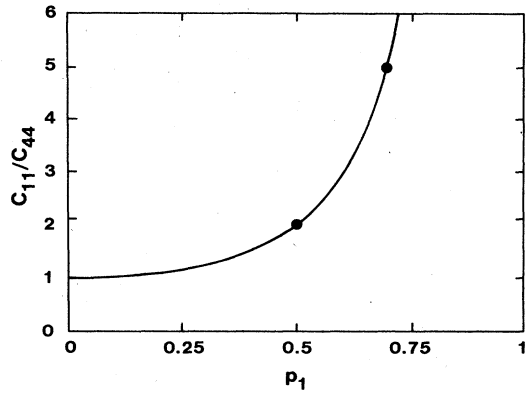

FIG. 8. EMT result for the value of C_{11}/C_{44} on the critical line shown in Fig. 2. The two circles at $C_{11}/C_{44}=2,5$ are the values on the critical line crossed by the tracks in Fig. 2.

to the simulations are impressive. We stress that there are *no* adjustable parameters. The agreement between the EMT and the simulations is as good as in I and perhaps more impressive because the elastic moduli are not all linear in p. There is considerable structure in the elastic moduli shown in Fig. 5, with some curves being concave upwards and some concave downwards.

The EMT predicts that the ratio C_{11}/C_{44} should go to a fixed value, independent of starting value of the ratio γ/α, as $p\to p^c$. This is shown in the flow diagrams of Figs. 6 and 7. In Fig. 8 we show the value of C_{11}/C_{44}, on the critical line, as a function of p_1 (with $p_1+p_2=\frac{1}{2}$). Thus the value of C_{11}/C_{44} is universal in that it does *not* depend on the starting *material parameters* α,γ. It does, however, depend on *geometry* and varies along the phase line separating the rigid and floppy regions in Fig. 2. Not surprisingly when $p_1=1$, $p_2=0$ we find that $C_{11}/C_{44}=1+\alpha_m/\gamma_m\to\infty$, while when $p_1=0$, $p_2=1$ we find that $C_{11}/C_{44}=1$ as shown in Fig. 8.

There is a rather curious symmetry present in the EMT equations for this lattice which results from Eqs. (19)—(22) being similar if the coordinate axes are rotated by 45° and $\gamma\rightleftarrows\alpha$, etc. In particular, it is easy to show that

$$a_1^*(\alpha_m/\gamma_m)=a_2^*(\gamma_m/\alpha_m)\ . \tag{31}$$

This implies that along the critical line

$$p_1^c(\alpha_m/\gamma_m)=p_2^c(\gamma_m/\alpha_m)\ , \tag{32}$$

and hence when $p_1^c=p_2^c$, we have $\alpha_m=\gamma_m$ or $C_{11}/C_{44}=2$ as shown in Fig. 6. The simulations appear to be consistent with this result. The simulation results became quite noisy near p^c as two small numbers are being divided. It becomes increasingly difficult to be sure that the systems are truly relaxed as p^c is approached. The long-time behavior of the elastic moduli seemed to follow

$$C(t)=C+A\exp(-\beta t)$$

and we used this to extract the desired asymptotic elastic modulus C. All the EMT elastic moduli shown in Figs. 4 and 5 come in linearly at p^c. In reality we would expect a critical region with an exponent different from 1, but our simulations would have to be averaged over many more configurations to obtain sufficiently reliable data in this region and to obtain a sufficiently good value of the C_{11}/C_{44} ratio on the critical line.

Track 2 (and subsequently track 3) was chosen so that the EMT value for $C_{11}/C_{44}=5$ was obtained as the critical line was crossed. Although the results in Figs. 6 and 7 become quite noisy as p^c is approached, we conclude that there are no systematic deviations from EMT within the noise limitations of the simulations.

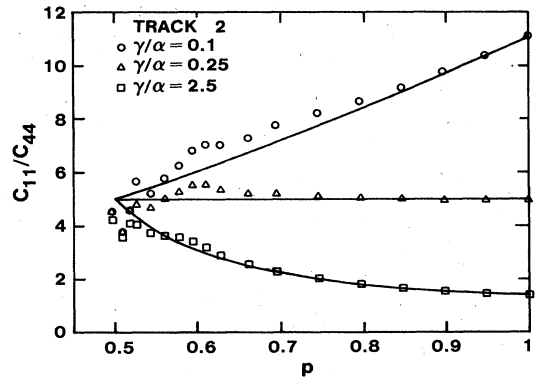

FIG. 7. Same as Fig. 6 except along track 2 [where $(1-p_2)=2.37(1-p_1)$].

VI. CONCLUSIONS

We have shown that EMT gives a quite remarkable description of networks with nearest-neighbor and next-nearest-neighbor central forces. The agreement is much better than in most other problems in which EMT has been used.[7] We know that EMT gives the initial slope correctly when only a few impurities are present, but it

usually only gives a rough estimate of p^c. In the present class of problems, the constraints argument leads to an excellent value for p^c. The EMT gives the same p^c as the constraints argument, and hence when the two ends of the curve are fixed, there is little margin for error. Nevertheless the agreement is quite remarkable. We do not know why the constraints argument is so accurate for random elastic networks. It is particularly important to understand this because of its potential importance in glassy networks.[2,5,8,9]

We caution the reader that there are actually *two* distinct classes of problems. In *class 1*, sufficient forces are specified so that the lattice is rigid if connected. Nearest-neighbor central and angular forces are sufficient to ensure this in two dimensions. The transition takes place at $p^c=p_c$ where p_c is the concentration of bonds present at ordinary *geometrical percolation* (denoted by the *subscript c*). Examples of such problems have been studied by various authors.[10–12] In *class 2*, geometrical connection alone is not sufficient to ensure that there is an elastic restoring force. Examples are the work of S. Feng, M. F. Thorpe, and E. J. Garboczi[1] (see also Refs. 12 and 13), and the work of this paper. As bonds are removed, "free hinges" are created which are ineffective in transmitting an elastic force. This is why the transition occurs at $p^c=\frac{1}{2}$ in this paper, whereas the percolation concentration for bonds with first- and second-neighbor connections in the square lattice[14] is close to $p_c=2/(z_1+z_2)=\frac{1}{4}$. For $\frac{1}{4}\leq p<\frac{1}{2}$ the lattice is geometrically connected but has no elastic properties. We may characterize class-2 problems by *rigidity percolation*[2] to distinguish them from class-1 problems that involve *connectivity percolation.*

The EMT predicts a universal value of the ratio of the longitudinal to the transverse sound velocities $v_l^2/v_t^2=C_{11}/C_{44}$ that depends only on the geometry (i.e., p_1,p_2) and *not* on the initial value of C_{11}/C_{44} when all bonds are present. A similar conclusion was reached by Bergmann,[10] who showed that $C_{11}/C_{44}\to 3.5\pm 0.2$ for the bond-diluted honeycomb lattice with nearest-neighbor central and angular forces (this system has a critical point rather than a line of critical points as in this work). Thorpe and Sen,[15] using EMT showed that if elliptical holes are cut randomly in an elastic sheet, then at the critical point the ratio C_{11}/C_{44} is independent of the material parameters but does depend on the aspect ratio of the elliptical holes. It has also been shown that the Born model has similar properties.[16]

It seems to us that there is now conclusive evidence that for both class-1 (see Ref. 10) and class-2 (as shown in this paper) problems, the ratio C_{11}/C_{44} reaches a universal value at the fixed point. This value is *independent* of the initial value of C_{11}/C_{44} but *dependent* upon geometry in the class-2 problem studied in this paper and probably quite generally. The work of this paper shows that the conjecture of Bergmann and Kantor[17] that $C_{11}/C_{44}\to 2$ for all two-dimensional systems is incorrect (this has also been shown by Bergmann[10]). The detailed local geometry is important and this number would be expected to be different for different geometries. The dilute honeycomb lattice[10] is always elastically isotropic (i.e., $C_{11}-C_{12}=2C_{44}$). In the present case the lattice is anisotropic. The system does *not* become isotropic on the critical line except at one isolated point of no particular significance. The phenomenological "node-link" model of Kantor and Webman,[18] assumes isotropy. It would be useful to extend this model to more general situations such as the one discussed here.

ACKNOWLEDGMENTS

One of us (M.F.T.) should like to thank Schlumberger-Doll Research for their hospitality. Many of the ideas in this paper concerning flow diagrams, fixed points, universal ratios, etc. were first discussed there with L. Schwartz, P. Sen, and S. Feng. The support of the ONR and NSF is gratefully acknowledged.

---

*Present address: Armstrong World Industries, Inc. Research and Development, P.O. Box 3511, Lancaster, PA 17604.

[1]Shechao Feng, M. F. Thorpe, and E. J. Garboczi, Phys. Rev. B **31**, 276 (1985).

[2]M. F. Thorpe, J. Non-Cryst. Solids **57**, 355 (1983).

[3]See, for example, C. Kittel, *Introduction to Solid State Physics* (Wiley, New York, 1966), p. 121.

[4]Cauchy's relations are discussed in A. E. H. Love, *A Treatise on the Mathematical Theory of Elasticity,* 4th ed. (Cambridge University Press, Cambridge, England, 1934).

[5]J. C. Phillips and M. F. Thorpe, Solid State Commun. **53**, 699 (1985).

[6]Dangling bonds and two coordinated bonds are removed by "trimming" as in I. The two coordinated sites with bonds at 180° are *imagined* to be slightly buckled to $180°-\Delta$, when they become "free hinges" and ineffective elastically and can be removed. This alleviates the necessity to actually buckle the lattice.

[7]See, for example, R. J. Elliott, J. A. Krumhansl, and P. L. Leath, Rev. Mod. Phys. **46**, 465 (1974); S. Kirkpatrick, *ibid.* **45**, 574 (1973).

[8]J. C. Phillips, J. Non-Cryst. Solids **34**, 153 (1979).

[9]H. He and M. F. Thorpe, Phys. Rev. Lett. (to be published).

[10]D. J. Bergman, Phys. Rev. B **31**, 1696 (1985).

[11]S. Feng, P. N. Sen, B. I. Halperin, and C. J. Lobb, Phys. Rev. B **30**, 5386 (1984).

[12]S. Feng and P. N. Sen, Phys. Rev. Lett. **52**, 216 (1984).

[13]M. A. Lemieux, P. Brenton, and A.-M. S. Tremblay, J. Phys. (Paris) Lett. **46**, L1 (1985).

[14]This approximation to p_c for bond percolation with first and second neighbors can be obtained from Eq. (30) with $d=1$.

[15]M. F. Thorpe and P. N. Sen (unpublished).

[16]L. Schwartz, P. N. Sen, S. Feng, and M. F. Thorpe (unpublished).

[17]D. J. Bergman and Y. Kantor, Phys. Rev. Lett. **53**, 511 (1984). These authors conjecture that for isotropic materials the ratio of the bulk modulus K to the shear modulus μ approaches the universal value $K/\mu=4/d$, where d is the dimension of the system.

[18]Y. Kantor and I. Webman, Phys. Rev. Lett. **52**, 216 (1984).